PCP
PLANT & CELL PHYSIOLOGY

Unveiling the molecular mechanisms of the stress resilience of High Arctic *Klebsormidium flaccidum*: a multifaceted study

Anastasiia Kolomiiets[1,2,3,*], Oleksandr Bren[2,3], Pavel Přibyl[3], Jana Kvíderová[2,3,4], Lenka Procházková[5], Ekaterina Pushkareva[6], Josef Elster[2,3,*] and Burkhard Becker[6,*]

[1]Department of Experimental Plant Biology, Faculty of Science, University of South Bohemia, Branišovská 1645/31a, České Budějovice, 370 05, Czech Republic, [2]Centre for Polar Ecology, Faculty of Science, University of South Bohemia, Na Zlaté stoce 3, České Budějovice, 370 05, Czech Republic, [3]Department of Phycology, Institute of Botany CAS, Dukelská 135,Třeboň, 379 01, Czech Republic, [4]Centre for Biology, Geosciences and the Environment, Faculty of Education, University of West Bohemia, Chodské náměstí 1, Plzeň, 306 14, Czech Republic, [5]Department of Ecology, Faculty of Science, Charles University, Albertov 6, Prague, 128 00, Czech Republic, [6]Institute for Plant Sciences, University of Cologne, Zülpicher Str. 47b, Cologne, 50674, Germany

*Corresponding authors: Burkhard Becker, E-mail, b.becker@uni-koeln.de; Josef Elster, E-mail, jelster@prf.jcu.cz; Anastasiia Kolomiiets, E-mail, anastasiia.kolomiiets@ibot.cas.cz

Received 11 April 2025; Accepted 1 August 2025

Abstract

The green alga *Klebsormidium* is found worldwide in terrestrial and freshwater habitats. A novel strain was isolated from biological soil crusts on Breinosa Mountain in Svalbard (High Arctic, 78°N) to investigate its adaptation to extreme Arctic conditions, characterized by low temperatures and short periods of snow-free ground. Genetic analyses confirmed the strain's identity as *Klebsormidium flaccidum*, showing high genetic similarity to strains from polar and temperate habitats. This study explored the effects of nitrogen starvation, cold stress, desiccation, and freezing, focusing on molecular responses and stress resilience. Nitrogen starvation strongly impacted metabolic activity, while cold and desiccation stress had more subtle effects, with *K. flaccidum* showing permanent stress-related gene expression instead of acute responses. Cold acclimation was found to enhance desiccation and freezing tolerance, while nitrogen starvation worsened the effects of these stresses. These results suggest that *K. flaccidum* CCALA 1182 is inherently capable of withstanding fluctuating environmental stresses, highlighting its potential for survival in diverse and harsh ecosystems.

Keywords: Arctic biocrusts • cold stress • cryo stress • desiccation • *Klebsormidium flaccidum* • nitrogen starvation

Introduction

Extreme environments range from aquatic and semi-aquatic to arid conditions, and vary in periodicity, amplitude, and regularity, initiating a range of ecological and physiological acclimations and adaptive responses. One of the most important ecological and physiological factors is the speed with which water can change from liquid to ice, snow, and complete dryness, especially at low or high temperatures. In this respect, polar environments represent one of the most extreme environments and provide similar stress in all polar regions. However, polar biocrusts have been found to exhibit high biodiversity (e.g. Rippin et al. 2019, Glaser et al. 2022, Mugnai et al. 2024, Pushkareva et al. 2024) and Elster and Benson (2004) suggested that the physical and chemical conditions of different locations have selected particularly resilient microbial strains (with their specific sets of adaptive biological traits).

Klebsormidium (*Klebsormidiophyceae*, Streptophyta) is one of the most widespread green algal genera found around the world in aero-terrestrial, terrestrial, and hydro-terrestrial habitats (Lokhorst 1996, Škaloud 2006, Rindi 2007, Silva et al. 1972, Sluiman et al. 2008, Elster et al. 2008a, 2008b, Ryšánek et al. 2016). The genus *Klebsormidium* is characterized by morphological and biological simplicity (simple construction of the thallus, unbranched uniseriate filament, with undifferentiated cylindrical cells possessing a single parietal plate- or disc-shaped chloroplast, and lack of information on sexual reproduction). Its high ecological importance in various marginal and/or extreme environments has made *Klebsormidium* a fascinating model organism to study the adaptation of microalgae to extreme environments (e.g. Elster et al. 2008a, 2008b, Holzinger et al. 2011, Rippin et al. 2019). Interestingly, despite its morphological simplicity, it shows a great intrageneric genetic diversity with apparently unique molecular adaptation strategies in different strains (Rippin et al. 2019).

The ability of some terrestrial streptophyte green algae to tolerate adverse conditions probably emerged during the transition from freshwater to terrestrial environments in the

Plant and Cell Physiology, 2025, 66(10),1397–1411. https://doi.org/10.1093/pcp/pcaf091, Advance Access publication on 6 August 2025, available online at https://academic.oup.com/pcp

evolution of land plants (Wang et al. 2020). This colonization was accompanied by the development of adaptations to the terrestrial environment (de Vries et al. 2016; de Vries and Archibald 2018; Wang et al. 2020), such as photoprotective mechanisms to counter excessive solar radiation and proteins that protect cells during dehydration, among many others (e.g. Becker and Marin 2009, Pierangelini et al. 2017, Becker et al. 2020). These adaptations are often shared with land plants and have most likely paved the way for the emergence of embryophytes (Holzinger et al. 2014, Becker et al. 2020).

The filamentous streptophytic green alga *Klebsormidium* has been extensively studied for physiological and structural responses to desiccation (Karsten et al. 2016) or low temperatures (Nagao et al. 2008), natural factors in soil crusts. A draft genome of *Klebsormidium nitens* is available (Hori et al. 2014). Ecological influences have been attributed to fine-scale structuring of genotypes and differentiation of cryptic species (Škaloud and Rindi 2013, Ryšánek et al. 2015). This study aimed to assess the molecular mechanisms underlying the freezing and desiccation tolerance of a *K. flaccidum* strain isolated from a biocrust in the High Arctic (Svalbard). Several studies have analyzed these stresses in terms of physiology (e.g. Elster et al. 2008a, 2008b, Karsten et al. 2016), while molecular studies have only addressed desiccation (Holzinger et al. 2014, Rippin et al. 2019) and cold stress (Rippin et al. 2019). In this study, we investigate the effect of nutrients on cold, desiccation, and cryo stress on *K. flaccidum* from Svalbard (High Arctic).

Results

Isolation, morphological description and identification of *K. flaccidum*

A filamentous green alga was isolated from biocrust samples collected near Longyearbyen (Svalbard, High Arctic). Axenic cultures were established and used for identification and characterization of the novel strain. The filaments of this novel strain were solitary, nonmucilaginous. Young filaments consisted of 4–7 cells, mature ones usually contained 10–17 cells (Fig. 1b). On the surface of the agar plates also, longer filaments developed that twist, forming bends and tangles (Fig. 1a).

The cells were predominantly cylindrical, except for the terminal ones in the filaments, which were rounded at the distal end (Fig. 1b). The cell wall was smooth, the chloroplast was parietal, grooved, green, or yellowish-green. Cells were 6.13–7.35 μm wide, with a length usually 2–3 times more than width, while young cells might be isodiametric. The investigated strain reproduced by mitotic cell division. Zoospores, aplanospores, and sexual reproduction were not observed in the culture.

Based on the 18S rRNA sequencing (1653 bp), the studied strain CCALA 1182 was identical for this marker with *K. flaccidum* ACSSI 009 (MK262905), *K. flaccidum* SAG 7.91 (EU434019) and *Klebsormidium* sp. ACSSI 294 (MT425959). Less related taxa (1 bp in conservative 18S rRNA gene sequence) were *Interfilum paradoxum* SAG 4.85 (EU434016) and *Klebsormidium dissectum* SAG 2155 (EF372518). Sequencing of the ITS2 marker (224 bp) revealed that the aforementioned strains of *K. flaccidum* ACSSI 009 and *K. flaccidum* SAG 7.91 differed from the new isolate only by 1 bp, and the type strain of *K. flaccidum* SAG 2307 differed from the studied alga only by 3 bp (no compensatory base change) (Supplementary Fig. S1), thus confirming that they represent one species. Consequently, CCALA 1182 was assigned to *K. flaccidum* (Silva et al. 1972).

Growth

Optimal values for temperature and light intensity were determined for *K. flaccidum* strain CCALA 1182 (Fig. 2). The strain showed a relatively wide range for both temperature and light intensity, achieving sufficient growth between ~14–27°C and 80—over 200 μmol m^{-2} s^{-1}, respectively. The optimum temperature was around 20–25°C; however, the optimum light intensity was not reached at the intensities tested, which appeared to be higher than 200 μmol m^{-2} s^{-1} (Fig. 2a). In addition, the time course of growth at different temperatures was examined for the near-optimal light intensity (Fig. 2b). Growth showed different patterns for each temperature; growth at all temperatures started with a lag phase. The length of the lag phase (between 1 and 4 days) was negatively correlated with temperature. The growth curve at 8°C was the only one that did not show the full sigmoidal pattern, but rather the first half of it, probably due to growth limitation during the limited time of the experiment. On the other hand, growth at 15 and 30°C reached the stationary phase after 8 and 3 days, respectively. The highest biomass was recorded at 22°C, reaching 3.7 g L^{-1} after 9 days and only entering the early stationary phase, suggesting further growth potential under these conditions. The temperature of 22°C was therefore considered to be the optimum temperature for this strain and was used as the reference condition in all further experiments.

Stress experiments—overview

To investigate the resilience of *K. flaccidum* CCALA 1182 from Svalbard to cold stress, N-limitation, desiccation, and freezing, we performed stress experiments and investigated the effect of N-limitation and cold stress on the overall survival rates after desiccation and freezing and performed a transcriptomic study of selected conditions yielding suitable total RNA. The general workflow is depicted in Fig. 3.

Viability tests

The cell viability of the culture and treatments was assessed using a multiparameter staining protocol. Figure 4 shows examples of the staining protocol used for different healthy and injured cells. Cells that were intact and active generally occurred in filaments of four cells or more, with a clearly visible healthy protoplast and the presence of pigments that could be observed in bright-field microscopy. The cell nuclei were intact and well-stained with DAPI, and some crystals of CTC-formazan were observed (Fig. 4, row 1). Metabolically active but injured cells also had pigments, but the protoplasts of some cells showed deformations. Such cells had positive SYTOX Green staining of nuclei, which indicated damage of the cell membranes, although at the same time respiratory activity continued (Fig. 4,

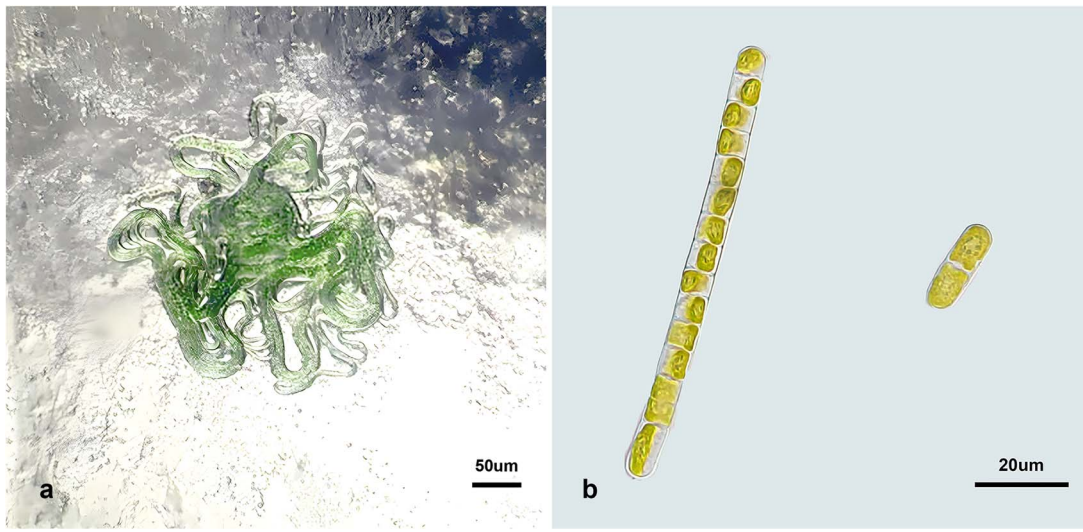

Figure 1. (a) Plexus of filaments of *K. flaccidum* on agar plates. (b) Mature and young filaments of *K. flaccidum*. Under unfavorable conditions (desiccation, cold), the filaments disintegrated into shorter fragments or even individual cells.

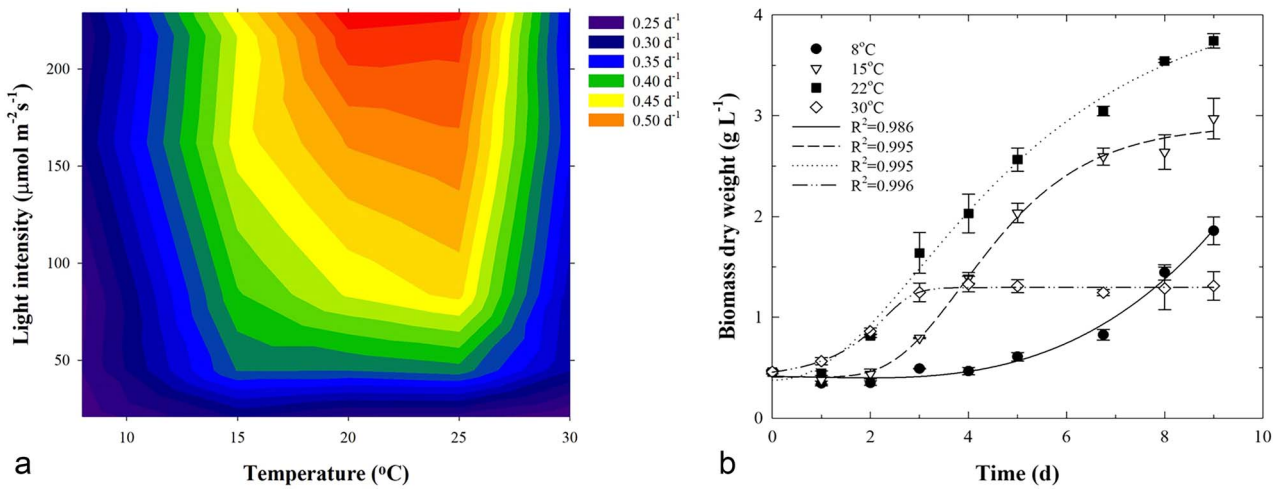

Figure 2. Effect of temperature and light intensity on growth of *K. flaccidum* CCALA 1182. (a) Contour plot showing the specific growth rates (based on biomass dry weight) of the strain CCALA 1182 after 6 days of cultivation at varied temperatures and light intensities. (b) Growth curves of strain CCALA 1182 at different temperatures and light intensity of 200 μmol m^{-2} s^{-1}. Data represent means and SD of three biological replicates.

row 2). Structurally intact metabolically inactive cells had nuclei stained with DAPI, but other dyes showed negative signals (Fig. 4, row 3). Metabolically inactive injured cells had well-stained nuclei by SYTOX Green and DAPI, but without CTC signals (Fig. 4, row 4). Dead cells showed no positive staining (Fig. 4, row 5).

The results of the viability tests are shown in Fig. 5, and a statistical analysis comparing all conditions is shown in Supplementary Figs S2–S4. At 22°C in the presence of nitrogen in the pretreatment, we observed a substantial damaging effect of desiccation. There was a 10-fold decrease in the proportion of metabolically active intact cells (P = .03) and an increase in metabolically inactive injured cells (2.8-fold, 50% of the cells, P = .09) and dead cells (3.2-fold, 13.5% of the cells, P = .09), suggesting that desiccation primarily disrupted cellular activity rather than causing mass cell death (Fig. 5, Supplementary Fig. S2).

In the absence of nitrogen at 22°C in pretreatment, we observed again a reduction of intact metabolically cells and intact inactive cells and a large increase of metabolically inactive and injured cells (20-fold, 59.5% of the cells), as well as dead cells (7.1-fold, 27.0% of the cells), however, all observed differences were not statistically significant (Fig. 5, Supplementary Fig. S2).

At +8°C, in the presence of nitrogen, the number of active, intact cells decreased (6-fold, 6.1% of the cells, P = .01). Applying desiccation of cells pretreated at 8°C with nitrogen, metabolically active injured cells were not detected (P = .01) and the number of injured inactive cells increased (1.5-fold, 35.3% of the cells, P = .07). The proportion of dead cells remained unchanged (P = .31) (Fig. 5, Supplementary Fig. S2).

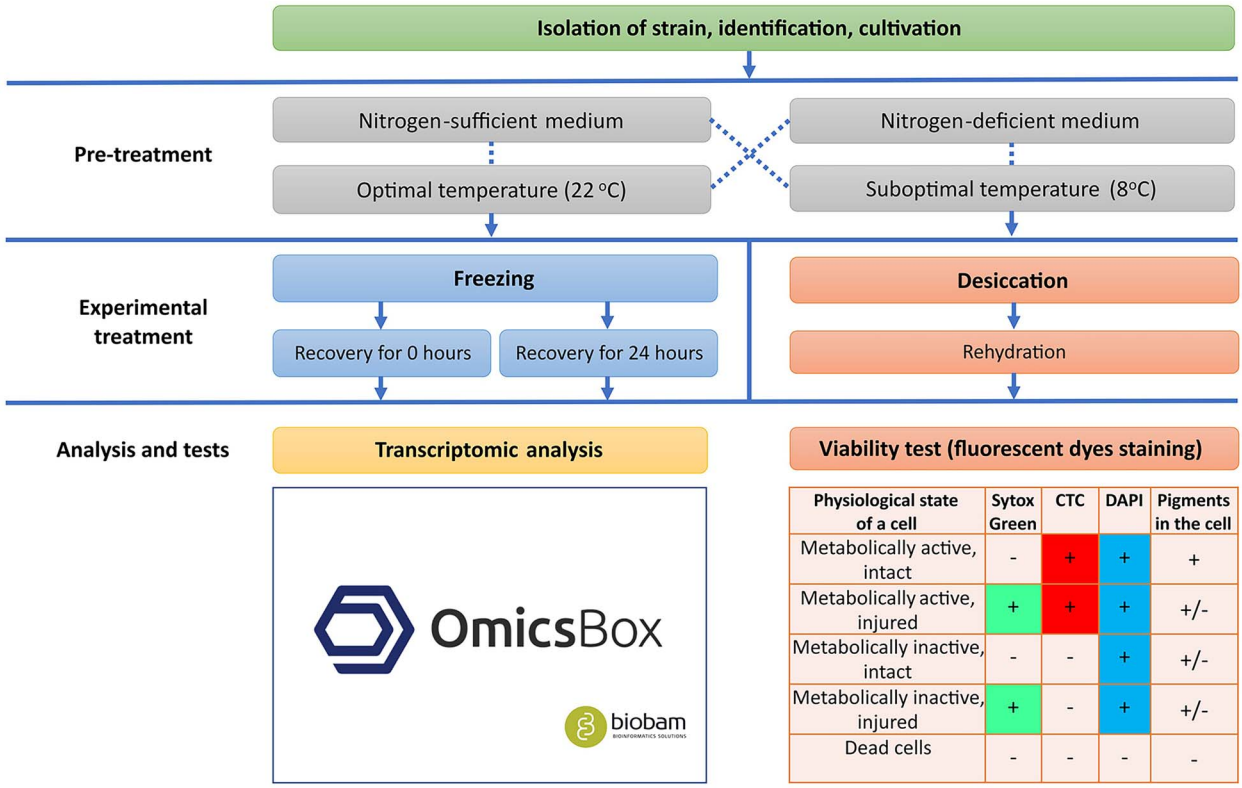

Physiological state of a cell	Sytox Green	CTC	DAPI	Pigments in the cell
Metabolically active, intact	-	+	+	+
Metabolically active, injured	+	+	+	+/-
Metabolically inactive, intact	-	-	+	+/-
Metabolically inactive, injured	+	-	+	+/-
Dead cells	-	-	-	-

Figure 3. Flow diagram of the experimental procedures to analyze stress resilience. Plus and minus indicate observed and absent staining of the cells, respectively, +/− indicate variable staining of the natural pigments.

Desiccation did not cause statistically significant differences compared with the control in cells pretreated at +8°C without nitrogen ($P > .05$). However, results showed no metabolically active intact cells and the largest number of dead cells (15.9%) compared with other treatments (Fig. 5, Supplementary Fig. S2).

Freezing affected cell viability, leading to an increased number of dead cells. This became more pronounced after the 24 hours recovery period and was stronger at 22°C (28.5% of the cells) than at 8°C (9.5%) and in the absence of nitrogen (57.9% at 22°C, 35.1% at 8°C), although these comparisons were often statistically not significant. However, for all pretreatments we observed an increase in injured metabolically active and/or inactive cells upon freezing. Both represented more than 94% of the cells, except for the pretreatment at 22°C with nitrogen, where 25.5% of the cells were immediately dead and 69% of the cells were injured. There was a decrease in the proportion of the metabolically inactive injured cells and increase in the dead cells, pretreated at 22°C with nitrogen after 24 hours of recovery following freezing. We observed a similar situation in the experiment with pretreatment at 8°C with nitrogen. After 24 hours, in the variant with pretreatment at 22°C without nitrogen, metabolically inactive injured cells almost completely transferred either into a metabolically inactive intact state or died (Fig. 5, Supplementary Fig. S2).

Pairwise comparison of cell viability in the experimental variant pretreated at 22°C showed that nitrogen promotes survival under adverse conditions. Variants with nitrogen showed fewer injured and dead and more intact cells. Statistically significant results at this pretreatment temperature were only in the freezing experiment (0- and 24-hours recovery) (Fig. 5, Supplementary Fig. S3).

A similar situation we noticed, comparing the experiments with pretreatment at 8°C. Comparison of controls ($P \leq .05$) indicates that nitrogen deprivation initiates the decrease of metabolically inactive intact cells (from 65.0% to 38.8%, $P \leq .05$). The proportion of inactive injured (23.0% vs. 45.3%, $P \leq .05$) and dead (5.7% vs. 15.9%, $P \leq .05$) cells increases. In addition, living, metabolically active, intact cells are completely absent without nitrogen ($P = .04$). However, comparison of viability in freezing did not result in significant changes in the proportions—statistically significant results were observed at 0 hours of freezing recovery for all injured and dead cells (Fig. 5, Supplementary Fig. S3).

Pairwise comparison of the experimental results (pretreatment with nitrogen) indicated the influence of temperature on the cell viability. A lower proportion of active intact cells is observed in the control at lower pretreatment temperatures (37.3% vs. 0.22%, $P \leq .05$). As noted earlier, low temperatures reduce metabolic activity, which is observed between controls with a higher proportion of intact metabolically inactive cells in between the controls (24.1% vs. 65.0%, $P \leq .05$), between the variants in the desiccation (29.9% vs. 55.9%, $P \leq .05$) and freezing (13.0% vs. 53.0%, $P \leq .05$) experiments. At the same time, it was found that lower pretreatment temperatures provide lower cell mortality and a lower proportion of metabolically inactive

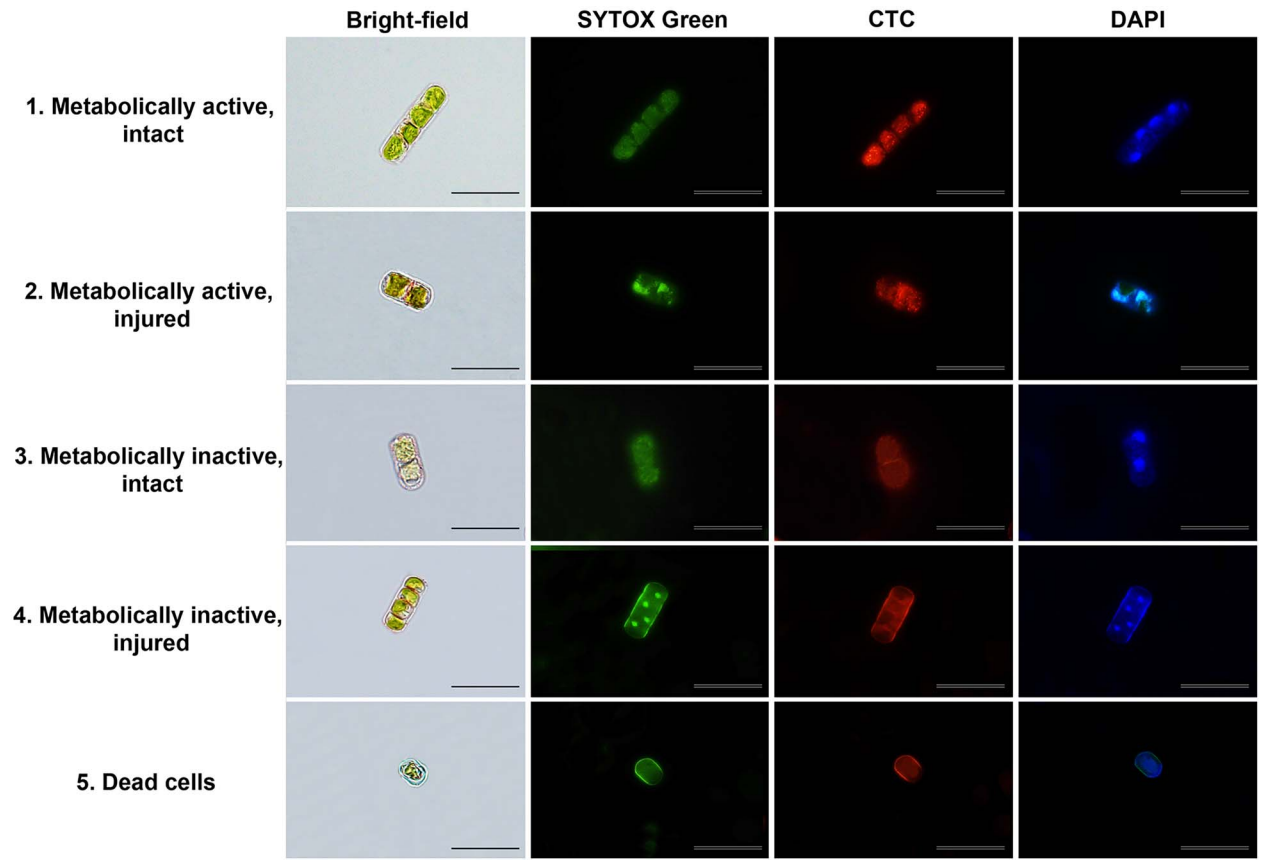

Figure 4. Cell morphology of *K. flaccidum* CCALA 1182. Rows represent viability states, columns—bright-field microscopy and staining with different dyes. Scale bars are 20 μm.

injured cells, which is observed in desiccation (13.5% vs. 8.8% and 35.9% vs. 25.3%, $P \leq .05$ both) and freezing (25.6% vs. 5.3% and 61.5% vs. 55.9%, $P \leq .05$ both) experiments. A similar trend is observed when comparing statistically significant variants of the results of the experiment with pretreatment at different temperatures, but without nitrogen (Fig. 5, Supplementary Fig. S4).

In agreement with the observed large number of dead or injured cells after desiccation and freezing under some conditions, total RNA of sufficient quality for further analysis could be isolated only from some experimental setups, allowing us to perform three different experimental comparisons using RNASeq. In the first experiment, we investigated the effect of cold stress (8°C) and N-limitation (full 2-factor design), in a second experiment *K. flaccidum* CCALA 1182 was exposed to desiccation stress at 22°C with/without nitrogen present in the medium (full 2-factor design), and finally, we investigated the effect of freezing on *K. flaccidum* CCALA 1182 (control, freezing, 24 hours recovery after thawing).

Transcriptomic analysis—overview

Transcriptomic sequencing of poly(A)-enriched RNA yielded between 24.5 and 60.4 million reads per sample. *De novo* assembly resulted in a total of 91 257 super-transcripts. Cluster analysis (96% identity) reduced the number of transcripts in the dataset to 48 803 with lengths up to 42 888 bp. The number of transcripts (and the large size of some transcripts) was still far higher than expected for a *Klebsormidium* sp. Completeness assessment using the Viridiplantae BUSCO database showed that the transcriptome represented ~84% of the genome (complete single copy or duplicated, Supplementary Fig. S5A). Open reading frame (ORF) analysis revealed 12 425 open reading frames, the majority (81.2%) of which were complete (Supplementary Fig. S5B). Diamond Blast analysis using a taxonomy filter set to Viridiplantae yielded 13 911 hits, almost all with either *K. nitens* (draft genome available, Hori et al. 2014) or *K. flaccidum* as top hits (Supplementary Fig. S5C). In the following, we present the results of the three experiments separately.

Cold stress and N-limitation

For this experiment, the cells were either cultivated at 22°C and 8°C, and in the presence (N+) or absence (N−) of nitrogen. The effects of the different treatments on differential gene expression are summarized in the principal component analysis (Fig. 6). The treatments were associated with huge changes in gene expression (between 1926 transcripts and 6134 transcripts showed differential gene expression in this experiment).

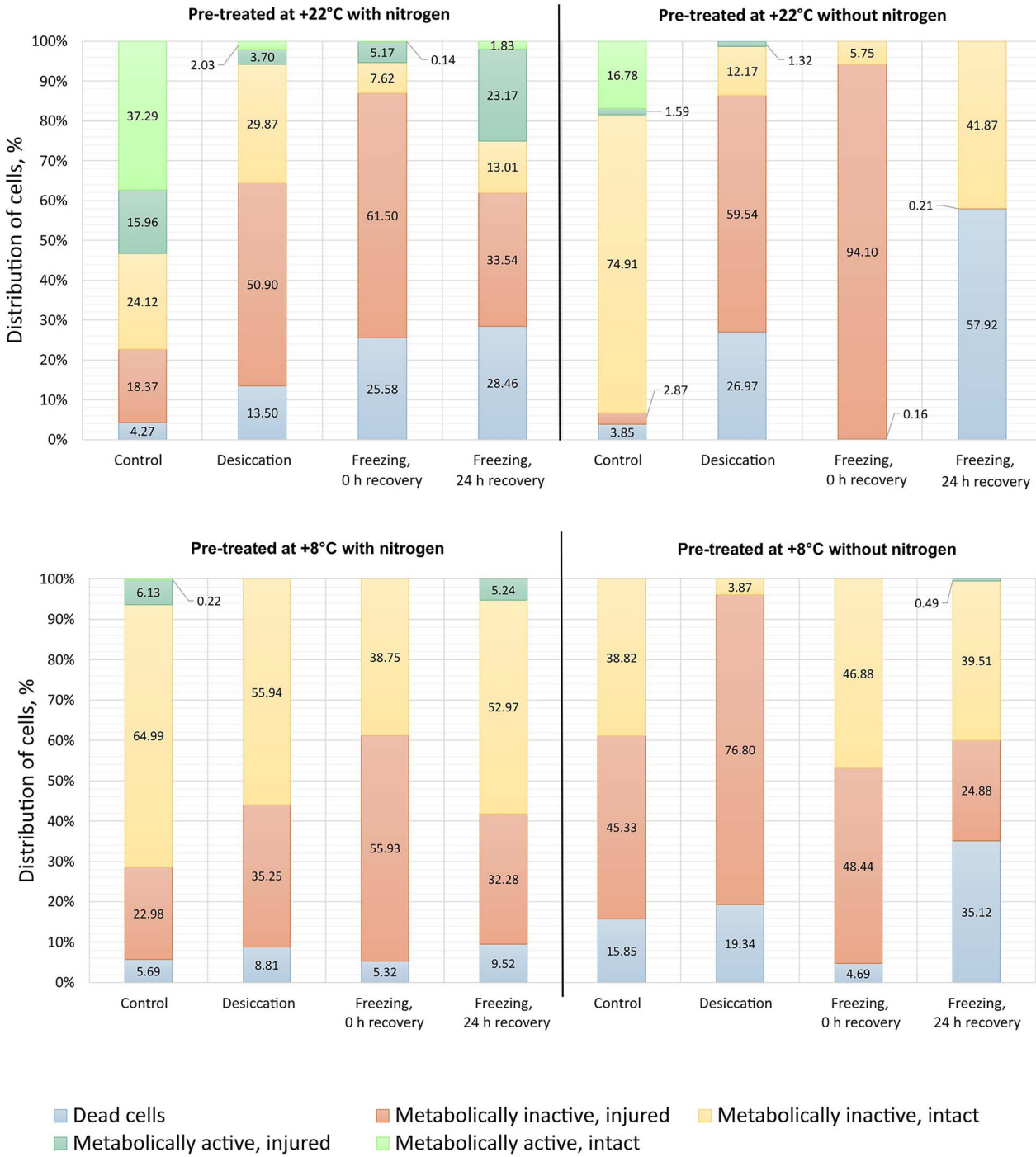

Figure 5. Cell viability after different experimental treatments. The distribution of cells by their viability status compared to control conditions is shown at optimal and suboptimal temperatures with and without nitrogen supply (control), and further experimental treatment by desiccation and freezing. Statistical tests comparing the different treatments and conditions are shown in Supplementary Figs S2–S4.

Overall, the effect of nitrogen limitation was stronger than the effect of cold stress (Fig. 6).

Most regulated transcripts showed a very clear differential gene expression pattern. Supplementary Fig. S6A shows the heat map and the clustering dendrograms for the 50 most strongly regulated transcripts (log2CPM expression values range from −4.72 to 14.09). The effect of N-limitation was the dominant clustering force. The temperature effect was much weaker but a bit stronger when nitrogen was present. The 50 transcripts are clustered in three major expression groups. Seventeen of the 50 proteins were hypothetical proteins with no clear function. The hypothetical proteins could be found in all major clusters. The major functions represented were transporters (8 transcripts, including several amino acid

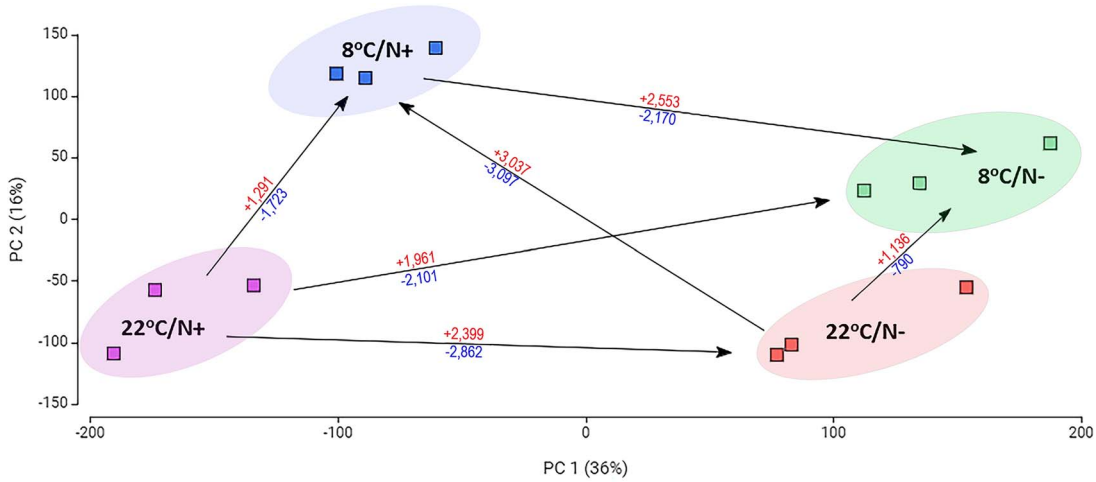

Figure 6. Principal component analysis plots showing the overall differences in gene expression of the triplicate samples upon experimental treatments: cultivation at 8° and 22°C and the presence or absence of nitrogen. Arrows and numbers indicate pairwise comparisons with the arrowhead pointing from the control to treatment and numbers above the arrow representing up-regulated transcripts and numbers below the arrow representing down-regulated transcripts. The number at axis name indicates the percentage of explained variation.

transporters), N-metabolism (5 including 3 acetamidase/formidase transcripts) and photosynthesis (12, with 8 *LHCA* transcripts). Several UDP-Glc-4 epimerase and a peptidylprolyl-isomerase were also present. Cluster 1 showed strong down-regulation at 22°C in the presence of nitrogen. It did not contain any photosynthesis-related genes, but many transporters and nitrogen metabolism-related genes. It might represent stress genes which were repressed at the optimal growth temperature and/or the presence of nitrogen. Clusters 2 and 3 contained many photosynthesis-related genes. In cluster 3, these genes were either strongly upregulated in the presence of nitrogen or strongly down-regulated upon nitrogen starvation.

Gene set enrichment analysis (GSEA) and combined pathway analysis (CPA) were used to get an overview of the processes that strongly reacted to cold stress and N-limitation. The results of the CPA are presented in Table 1 and detailed maps of the regulated pathway with heat maps for the detected enzymes are presented in Supplementary Fig. S8A–G. N-limitation led to clear effects. In CPA, biosynthetic pathways for porphyrins and some core pathways (glycolysis, Calvin cycle, di- and tricarboxylate metabolism, pentose-phosphate pathway) were shut down, and N-assimilation was up-regulated. There were some other pathways which were also highlighted in the CPA with a Fisher's *P*-value below .05 but an FDR above .05, including ascorbate and aldarate metabolism, starch and sucrose metabolism (both down-regulated), and biosynthesis of unsaturated fatty acids (up-regulated). The only up-regulated functions in CPA were transcripts associated with nitrogen metabolism. Interestingly, *K. flaccidum* CCALA 1182 seemed to lack any known nitrate reductase transcript, although nitrate/nitrite transporters and other components for N-assimilation were present (Supplementary Fig. S8G). Supplementary Fig. S7A and B shows the biological processes obtained by GSEA as word clouds, mainly reflecting the effect of nitrogen starvation. Photosynthesis-related terms were enriched among down-regulated transcripts, whereas potassium-transport and signal-transduction pathways were enriched in up-regulated transcripts. Surprisingly, neither CPA nor GSEA showed typical pathways known to be up-regulated in cold stress, such as ROS metabolism, changes in fatty acid composition or biosynthesis of osmolytes. However, it should be noted that CPA returned biosynthesis of unsaturated fatty acid as an up-regulated process, but with an FDR above .05.

Desiccation and N-limitation experiment

K. flaccidum CCALA 1182 was cultivated at 22°C in the presence (+N) or absence (−N) of nitrogen, followed by desiccation. The observed differential gene expression is summarized in Fig. 7. The variation within the desiccated samples was much higher than in the control samples, however, we still observed large differences. Between 2476 and 11 095 transcripts showed differential gene expression, with the effect of desiccation always stronger than N-limitation.

Most regulated genes again showed a very clear differential gene expression pattern. Supplementary Fig. S6B shows the heat map (log2CPM range from −4.55 to 13.93) with a clear effect of N-limitation and desiccation stress. Again, the effect of nitrogen starvation was the major clustering force; however, in contrast to cold stress, desiccation stress was clearly visible, especially under nitrogen starvation conditions. Similarly to the first experiment, several clusters among the 50 most regulated transcripts were related to photosynthesis (20 with 11 of them coding for *LHCAs*), in addition, enzymes from various classes maintaining cellular redox state, potassium transporters, N-metabolism enzymes (acetamidase/formamidase) were present. Again, a large number of transcripts (18) were identified as hypothetical proteins. There were three major clusters differing in expression. Cluster 1 contained transcripts down-regulated in the presence of nitrogen without desiccation stress.

Table 1. Up- (top) and down-regulated (bottom) pathways upon cold stress and N-limitation

Pathway	KEGG ID	GSEA Tag	GSEA NES	Fisher FDR	Fisher *P*-value
Pentose phosphate pathway	ko00030	BOTTOM	−2.8918364	2.94E-04	4.43E-06
Carbon fixation by Calvin cycle	ko00710	BOTTOM	−3.7322154	8.23E-09	2.48E-11
Fructose and mannose metabolism	ko00051	BOTTOM	−2.7751837	0.00645259	1.75E-04
Glycolysis/gluconeogenesis	ko00010	BOTTOM	−2.0366323	3.92E-04	7.09E-06
Glyoxylate and dicarboxylate metabolism	ko00630	BOTTOM	−2.3161852	1.13E-05	1.02E-07
Porphyrin metabolism	ko00860	BOTTOM	−3.5576155	3.32E-05	4.00E-07
Nitrogen metabolism	ko00910	TOP	2.0129993	0.00517703	1.25E-04

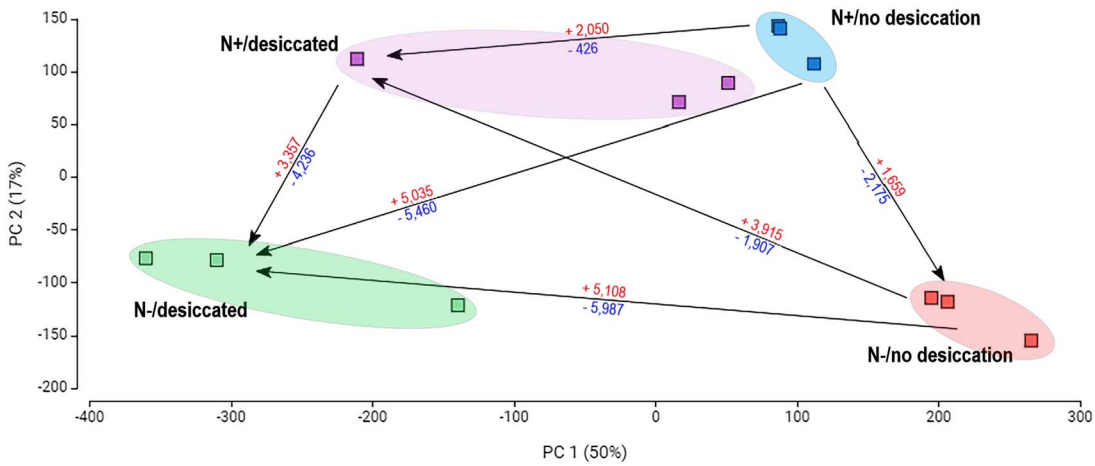

Figure 7. Principal component analysis plots showing the overall differences in gene expression of the triplicate samples upon experimental treatments: presence or absence of nitrogen and desiccation. Arrows and numbers indicate pairwise comparisons with the arrowhead pointing from the control to treatment and numbers above the arrow representing up-regulated transcripts and numbers below the arrow representing down-regulated transcripts.

These transcripts again included potassium transporters and nitrogen metabolism-related genes. A subcluster contained proteins which were down-regulated without desiccation stress and up-regulated upon applied stress. Two of them were hypothetical proteins and the other one represented a NADPH quinone reductase QORA, an enzyme well known to be involved in ROS protection. Cluster 2 was down-regulated upon nitrogen starvation and included mainly transcripts coding for hypothetical proteins. Cluster 3 was up-regulated in the presence of nitrogen and down-regulated to various degrees upon nitrogen starvation. Most of the photosynthesis-related genes were found in this cluster.

CPA returned 10 pathways with a Fisher's *P*-value below .05, however, all of them had an FDR of .08–.25. Most of them were the same pathways as found in the first experiment and might reflect N-starvation: amino acid metabolism, sulfur, biotin, and carbohydrate metabolism, Calvin cycle, and aminoacyl-tRNA biosynthesis. Arginine biosynthesis was among the up-regulated pathways. GSEA analysis (Supplementary Fig. S7C and D) showed the strong down-regulation of photosynthesis-related processes (Supplementary Fig. S7D) and an increase in protein catabolism as well as energy production (Supplementary Fig. S7C).

Freezing and thawing experiment

For this experiment, the cells grown at 22°C under nitrogen supply were slowly cooled down (0.143°C min^{-1}) to −40°C to mimic freezing occurring under natural conditions. The cells were thawed for immediate processing or were left for 24 hours for recovery and further processing. The effect of the experimental treatments on gene expression is shown in Fig. 8. Comparison of the gene expression after 24 hours of recovery and control cells still showed large differences, indicating that the cells did not fully recover. In the following, we first compare the effect of freezing, then the effect of recovery and finally, we present a comparison of cells after 24 hours of recovery with control cells.

Effect of freezing

The effect of freezing was clearly seen in a heat map (log2CPM values range from 9.52 to −4.35; Supplementary Fig. S6C). The heat map revealed three major expression groups; 30 of the 50 most strongly regulated transcripts were hypothetical proteins. The remaining proteins represented a mixture of functions, with two homologs of LEA proteins, generally involved in desiccation stress, but here down-regulated upon freezing, several

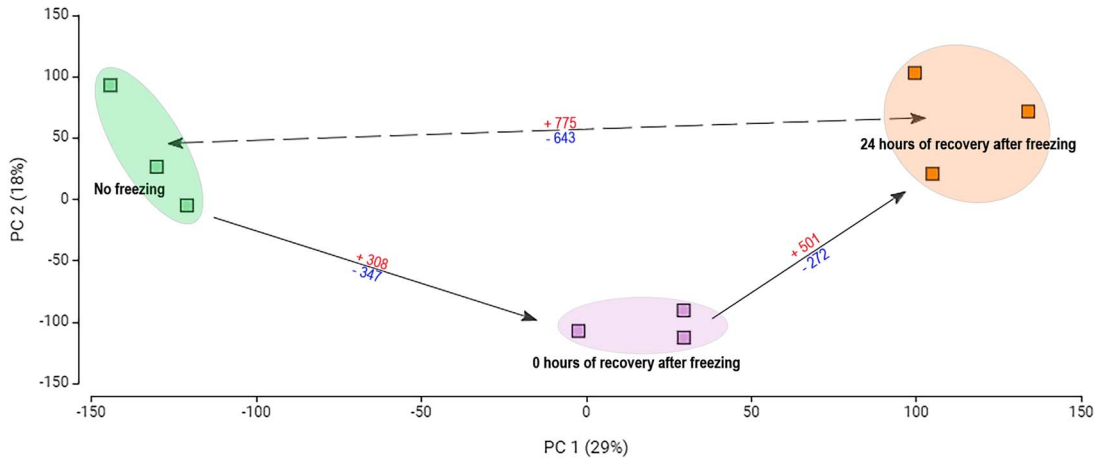

Figure 8. Principal component analysis plots show the arrangement of groups of samples following the effect of experimental treatment: cultivation under 22°C with nitrogen supply with further freezing and isolation of RNA after 0 and 24 hours of recovery. Arrows and numbers indicate pairwise comparisons with the arrowhead pointing from the control to treatment and numbers above the arrow representing up-regulated transcripts and numbers below the arrow representing down-regulated transcripts. Solid arrows indicate the time flow of the experiment. The dashed arrow indicates the comparison between the starting and end conditions.

oxidoreductases, but also transcripts involved in chromosome condensation and a vacuolar iron-transporter. CPA returned several pathways, but all with an FDR above 0.19. GSEA revealed cell cycle regulation to be up-regulated (Supplementary Fig. S7E) and photosynthesis, oxidative stress to be down-regulated (Supplementary Fig. S7F).

Recovery

The recovery of *K. flaccidum* cells from freezing led to changes in gene expression. After 24 hours, 773 transcripts showed a change in expression level when compared with freezing (Fig. 8). CPA returned only one significant pathway. Oxidative phosphorylation was up-regulated during recovery (Supplementary Fig. S8H). This was also evident from GSEA, which also showed an up-regulation for translation, protein maturation, and other basic cellular functions (Supplementary Fig. S7G), while RNA-related processes and cell cycle control were down-regulated (Supplementary Fig. S7H). The heat map (log2CPM values range from 11.06 to −4.42) showed 4 major clusters; 29 transcripts coded for hypothetical proteins (Supplementary Fig. S6D). Cluster 1 contained transcripts that were strongly expressed under both treatments but had higher expression rates at 24 hours of recovery. Cluster 1 transcripts encoded for chaperones, other proteins involved in protein maturation, but also a transporter and a Zinc-finger protein among others. Cluster 2 contained transcripts that were strongly down-regulated during freezing and included mainly hypothetical proteins. Cluster 3 included transcripts that were slightly up-regulated during recovery, while Cluster 4 showed a very mixed regulation pattern. Both clusters contained the bulk of transcripts encoding hypothetical proteins.

Comparison of 24 hours recovery with control

To see whether the cells were back to their normal gene expression pattern after 24 hours of recovery, we compared the gene expression pattern between control cells and cells after freezing and 24 hours of recovery. More than 1400 genes still showed a differential gene expression (Fig. 8). CPA again returned only oxidative phosphorylation as an up-regulated process (Supplementary Fig. S8I). Glycolysis and pyruvate metabolism were returned as down-regulated with a Fisher's *P*-value $< .05$, but had a high FDR of .32. GSEA analysis confirmed oxidative phosphorylation was the major up-regulated process (Supplementary Fig. S7I). Other up-regulated processes were cytoskeleton-dependent intracellular transports (Supplementary Fig. S7I), while down-regulated processes were again RNA-catabolic processes, and Acetyl-CoA involving processes (Supplementary Fig. S7J). A heat map (log2CPM values range from 9.31 to −4.30) is shown in Supplementary Fig. S6E. The transcripts clustered in four major expression groups and 29 transcripts again encoded for hypothetical proteins. Cluster 1 contained transcripts which were still down-regulated when compared with the control conditions and encoded proteins such as the two LEA proteins and the iron transporter, which were down-regulated during freezing, indicating that the cells had not reached their normal stress protection level. Cluster 2, which was up-regulated, compared to control conditions encoded for diverse proteins among them several involved in ATP production. Clusters 3 and 4 contained transcripts that were only weakly expressed under control conditions and showed diverse levels of regulation at 24 hours of recovery. Cluster 3 (two hypothetical proteins) had an even lower expression during recovery, while cluster 4 transcripts always had a higher expression level during recovery. The latter encoded for diverse functions but also contained several hypothetical proteins.

Discussion

K. flaccidum is the type species of the genus *Klebsormidium* (Silva et al. 1972). It has been found all over the world with a

distribution in terrestrial and freshwater habitats where it may form ecophysiologically distinct ecotypes (Karsten et al. 2016). Here, a new strain was isolated from Breinosa mountain on Svalbard (High Arctic, 78°8′47.40″N 16°2′21.50″E, 519 m a.s.l.) to investigate the adaptation of *Klebsormidium* to extreme Arctic conditions. At this height, the conditions are even more extreme than close to the sea and the soil is only snow-free for ∼60 days from July to September. The coldest month is March with an average air temperature of −17.7°C, the warmest month is July with an average air temperature of 6.3°C (Pushkareva et al. 2024, Hejdukova et al. in preparation). The isolated strain was identified to be a new isolate of *K. flaccidum* (identical 18S rRNA gene sequence, only 1–3 bp differences in the ITS2 region to other sequenced strains of *K. flaccidum*). The most closely related strains (1 bp difference in ITS2) originated from the former Union of Soviet Socialist Republics, the habitat was reported to be chestnut soil, freshwater habitat, and arable chernozem, respectively (Karsten et al. 2016). Moreover, 12 strains and environmental clones were 100% identical with our alga for the ITS2 molecular marker, which was suitable for identification on the species level. These algae were sampled from surface soil (0–5 cm) in Meseta mountain crest on Fildes Peninsula on King George Islands in Antarctica (Rybalka et al. 2023), bark surface of *Fagus sylvatica* in Hainich-Dün in Thuringia in Germany (Dreyling et al. 2022), and alpine biological soil crust on rock in the Tyrolean Alps in Austria (Mikhaiyluk et al. 2015) confirming the ubiquitous distribution of *K. flaccidum*. Whether different isolates of this species show genetic adaptations to their local environment or can tolerate a wide range in the abiotic conditions and how they achieve this is currently not clear. In this study, we investigated the stress resilience to cold, desiccation, N-starvation, and freezing stress of one isolate from a polar soil crust with physiological and molecular methods.

Nitrogen starvation

In all our experiments, nitrogen starvation had the strongest effect from all tested factors. Cells became metabolically inactive (Fig. 5) and in both experiments analyzed by transcriptomics, it was the major clustering force. Due to the sensitivity of the cells to light under nitrogen starvation conditions, we had to perform the nitrogen starvation experiment at low light intensity, the effect was clearly visible in our transcriptomic analysis. Photosynthesis-related transcripts were among the major regulated transcripts, showing a much higher expression in the control cells than in the starving cells (Fig. 8). For this reason, it remains unclear whether the observed down-regulation of photosynthesis-related transcripts was only due to the light, but also due to nitrogen starvation as photosynthesis is probably the cellular process in photoautotrophic cells requiring most of the cellular nitrogen. In plant leaves, up to 75% of the cellular nitrogen was used for photosynthesis (Zhuo et al. 2024), suggesting that a down-regulation of photosynthesis genes during N-starvation is very likely. The observed up-regulation of arginine biosynthesis under nitrogen starvation conditions in the desiccation experiment was interesting in this respect, as it might be expected that this process would be down-regulated too. However, arginine biosynthesis-controlled chlorophyll biosynthesis in cyanobacteria and green microalgae (Aigner et al. 2022, Kiss et al. 2023), and cells might try to maintain a certain amount of photosynthesis even under N-starvation to keep photosynthetic energy production going to a certain extent. Nitrogen starvation also strongly influences cytosolic osmolarity and it has been shown that *Chlamydomonas* compensated for this with potassium requiring the potassium channel KCN11 (Xu and Pan 2020). Interestingly, in both experiments, GSEA revealed potassium transport to be up-regulated and two potassium channels were up-regulated and among the 50 most regulated transcripts.

Cold stress

Growth experiments showed that the new isolate was not a psychrophilic but a mesophilic organism, indicating that the low temperature of Svalbard induces cold stress on this species. This was in agreement with Rippin et al. (2019), who observed that another strain of *K. flaccidum* and *K. dissectum* isolated from Antarctica and the High Arctic, respectively, were also mesophilic. However, soil surface measurements have consistently shown that biocrusts are exposed to much higher soil surface temperature during the short summer and we measured up to 13.5°C for the soil surface in July 2023 at the site of origin for our isolate (Pushkareva et al. 2024). Thus, *K. flaccidum* most likely grows mainly during the few warm summer days and is inactive during most of the year. This was supported by our viability tests, which indicated that at 8°C most of the cells were metabolically inactive (Fig. 5).

One of the more surprising results of this study was that upon cold treatment, we did not see any strong transcriptomic changes regarding ROS, osmolytes, and lipids composition, all well-known changes accompanying cold stress (Manasa et al. 2022). Our results suggest that *K. flaccidum* CCALA 1182 permanently expresses stress-related genes to be prepared for cold and desiccation stress which might also occur frequently during the short summer season in the High Arctic, especially at 500 m a.s.l. This was also in agreement with our transcriptomic data for the freezing recovery experiment. During freezing, LEA proteins involved in desiccation stress (Becker et al. 2020) were down-regulated, and immediately up-regulated during recovery, suggesting that these proteins served as a permanent factor in stress resilience. However, why LEA proteins were then down-regulated during freezing at all is currently not clear and is an interesting question requiring further studies.

Desiccation stress

Desiccation stress induces the same molecular stress and therefore the same reaction (increased osmolytes, ROS protection, and modification of fatty acid composition) as cold stress. For this reason, it was not surprising that cold acclimation has been found to have a positive effect on desiccation stress in *Klebsormidium* (Rippin et al. 2019). Our experiment supports the positive effect of cold acclimation, as cells grown at 8°C showed a reduced number of dead cells and inactive, injured cells upon desiccation. However, this was only the case if cells were not

starved. Osmolytes might play an important role in this, as a positive correlation between desiccation tolerance and polyols (arabitol, mannitol, and erythritol) amount was reported in three terrestrial *Trentepohlia* species (Holzinger et al. 2023). Up-regulated ROS protection, changes in osmolytes, and lipid composition have also been reported in other transcriptomic studies (*Klebsormidium*: Rippin et al. 2019, *Zygnema*: Rippin et al. 2017). However, again, we did not see a typical plant-like reaction in our experiments, supporting the concept that *K. flaccidum* CCALA 1182 might express stress-related proteins permanently. Two closely related desert and aquatic *Scenedesmaceae* species shared up-regulation of genes for protective proteins (Peredo and Cardon 2020). However, an extensive down-regulation of genes associated with diverse metabolic processes toward energy-saving mechanisms was specific for this desert, desiccation-tolerant species (Peredo and Cardon 2020). In contrast, related *Klebsormidium* species showed very different regulation patterns (Rippin et al. 2019), which agreed with the current study.

Freezing/thaw stress

Freezing led to many cryoinjured cells under all conditions, however, many more died under N-starvation. Often, nutrient limitation is considered to be a major factor in hardening for winter survival, however, there is not much evidence for this in the scientific literature. N-limitation has been shown to increase desiccation resilience in zygnematophycean algae (Pichrtová et al. 2014) and for some species of pine, the improved frost resistance of seedlings correlated positively with low N availability (Toca et al. 2018). Our results did not support hardening by nitrogen starvation but instead pointed to acclimation to low temperatures as a major factor in surviving freezing (Fig. 5). In agreement with our data, freezing tolerance was also significantly enhanced by cold treatment (2°C compared to 18°C) in a different strain of *K. flaccidum* (Nagao et al. 2008). The freezing tolerance positively correlated with the accumulation of soluble sugars (glucose and sucrose), a putative glycoside and amino acids, including GABA (Nagao et al. 2008). Conversely, it was shown that cold acclimation (+4°C) did not improve frost (−9°C) hardiness in either alpine or lowland *Mougeotia* species, *Mougeotia disjuncta* and *Mougeotia scalaris*, respectively (Permann et al. 2024). Among selected members of all streptophyte main lineages, *Klebsormidiophyceae*, represented by *K. nitens*, showed significantly higher tolerance to induced desiccation (Arzac et al. 2023). After desiccation, the content of polar lipids decreased in all studied species of Streptophyta. However, contrary to other Streptophyta, *K. nitens* was able to keep the galactolipid composition stable, except for decreased MGDG (Arzac et al. 2023), suggesting a role of thylakoid membrane integrity in desiccation tolerance.

Conclusion and Perspectives

In conclusion, this study highlights the complex molecular strategies employed by *K. flaccidum* CCALA 1182 to cope with extreme environmental conditions. While nitrogen starvation significantly affected metabolic activity, cold and desiccation stress appeared to have more subtle effects, with the organism exhibiting permanent stress-related gene expression rather than acute responses. Interestingly, the study found that cold acclimation positively affected desiccation and freezing tolerance, whereas nitrogen starvation increased the deleterious effects of desiccation and freezing stress. Our results suggest that *K. flaccidum* CCALA 1182 may be inherently prepared to withstand fluctuating environmental stresses, further highlighting its potential for survival in diverse, harsh ecosystems. Finally, the large number of hypothetical proteins that show large changes in expression levels upon stress indicates that we still know little about the mechanisms by which organisms such as *Klebsormidium* survive in the extreme conditions of their natural habitat. This is especially true for freeze/thaw tolerance, which is expected to become more common in Svalbard due to ongoing climate change.

Materials and Methods

Site description and sampling

Biological soil crusts (biocrusts) were collected on Breinosa mountain (78°8′47.40″N 16°2′21.50″E, 519 m a.s.l.) in the vicinity of Longyearbyen (Svalbard, Norway) in August 2022. The site and climate characteristics were described in Pushkareva et al. (2024).

Isolation and identification of a novel strain of *K. flaccidum* from Svalbard Gast

K. flaccidum (strain CCALA 1182) was isolated from the collected biocrust. All the samples collected in the field were transported and stored at −40°C in plastic zip-bags. The frozen sample was extracted from the freezer and quickly thawed under warm running water at a temperature +30–35°C for 5 minutes. Then, we manually homogenized the sample inside the zip-bag and placed 3–5 g of the soil on an agar plate, evenly distributing the soil particles over the surface of the nutrient medium with a sterile spatula (BG-11 medium, 1.5% agar). Plates were incubated for 2 weeks at 10°C and 10 μmol m^{-2} s^{-1} light intensity. Agar plates were checked by light microscopy (Amplival, Carl Zeiss Jena, Germany); grown uni-algal colonies were picked with a needle under a binocular (Zeiss, Germany); and transferred to a new agar plate. After 7–10 days, the strain was transferred to an Erlenmeyer flask filled with Z mineral growth medium (Staub 1961) and grown at 20°C and 25 μmol m^{-2} s^{-1} light intensity until a dense culture was obtained. The flasks were shaken manually several times a day. The culture was centrifuged (1000 g, 10 min, RT), the supernatant was discarded and the upper layer of the pellet was washed with sterile Z medium. The remainder of the pellet was resuspended in Z medium. This procedure was repeated twice to reduce any possible contamination. The resulting culture was diluted to a cell density of ∼1000 cells per ml (Bürker haemocytometer), plated on a new agar plate (1.5% agar in Z medium) and grown at 20°C and 25 μmol m^{-2} s^{-1} light intensity until colonies were obtained. Axenic colonies were selected by light microscopy (Amplival, Carl Zeiss Jena, Germany) and transferred to a fresh agar plate. The axenicity of the strain was checked by growing the strain on organic medium (1.5% agar in Z medium with 2% glucose). For long-term culture, the strain was maintained on an agar slant (1.5% agar in Z medium) at 10°C and light intensity of 10 μmol m^{-2} s^{-1}. The strain is deposited in the Culture Collection of Autotrophic Organisms (CCALA, https://ccala.butbn.cas.cz/index.php) as CCALA 1182.

Identification of *K. flaccidum* was performed using light microscopy of the sample and in culture (isolate) (Ettl and Gärtner 1988). To confirm the

taxonomic assignment, total DNA of the strain CCALA 1182 was extracted following the standard protocol in the DNeasy Plant Mini Kit (Qiagen, Germany) with the modification described in Procházková et al. (2018). The 18S small subunit ribosomal RNA gene sequence (18S rRNA) and internal transcribed spacer 2 sequence (ITS2) were amplified from DNA isolates by polymerase chain reaction using existing primers; for 18S rRNA: EAF3 (TCGACAATCTGGTTGATCCTGCCAG, Pröschold et al. 2001), BR5 (CCCGGGATCCAAGCTTGATCCTTCTGCAGGTTCACCTAC; Marin et al. 1998), 300F (GGAGAATTAGGGTTCGATTCCGGAG; Marin et al. 1998), for ITS2: 5.8SbF (CGATGAAGAACGCAGCG; Mikhailyuk et al. 2008) + AB28 (GGGATCCATATGCTTAAGTTCAGCGGGT; Curran et al. 1994). Amplification and sequencing reactions for these markers were done as described by Procházková et al. (2018). The obtained sequences of the strain CCALA 1182 were submitted to the National Center for Biotechnology Information (NCBI) Nucleotide sequence database (18S rRNA gene sequence: PV265869; partial 5.8S + ITS2+ partial 26S rDNA: PV275026). Secondary structure prediction of ITS2 was performed using the Mfold server in the same manner as in Procházková et al. (2018).

Growth conditions

Strain CCALA 1182 was transferred from the agar slant to an Erlenmeyer flask filled with 1/2 SŠ medium (Přibyl et al. 2015) and grown at 20°C and a light intensity of 25 μmol m^{-2} s^{-1}, shaken manually several times a day. The resulting cultures were grown in a bubble column cultivator, the design of which was described previously (Střížek et al. 2023). The setup parameters were as follows: 1/2 SŠ medium, temperature 20°C, light intensity gradually increased from 20 to 200 μmol m^{-2} s^{-1}, for 5 days. The resulting culture was used as seed for further experiments. The following combinations of light intensities and temperatures were tested for optimal setting of cultivation parameters: 21, 45, 84, 162, 217, and 229 μmol m^{-2} s^{-1} and 8, 15, 20, 25, and 30°C; 1/2 SŠ medium was used and columns were bubbled with 1% CO_2 in air in all variants. Three biological replicates were analyzed for each condition. Dry weight was determined by the gravimetric method at the beginning and after 6 days of the experiment, and specific growth rate was calculated as previously described (Přibyl and Cepák 2019). Similarly, growth curves at 8, 15, 22, and 30°C for the light intensity of 200 μmol m^{-2} s^{-1} were estimated by daily sampling during the 9 days of the experiment.

Algal cultures for the experiments were grown at either 22°C or 8°C, in 1/2 SŠ medium or 1/2 SŠ medium without nitrogen. The light intensity was set to 200 μmol m^{-2} s^{-1} for experiments with nitrogen, or 50 μmol m^{-2} s^{-1} for experiments without nitrogen. All variants (each 100 ml) were bubbled with 1% CO_2 in air and grown for 1 week.

Desiccation treatment and variable chlorophyll fluorescence measurements

Cultures were harvested by centrifugation (1000 g, 8 min, 15°C), the pellet was transferred to the Synpor membrane filter (diameter 50 mm, pore size 0.85 μm) using 1 ml of dH_2O, and ~1 ml of liquid was removed by vacuum filtration (EMD Millipore XX10 047, USA). The filters were then immediately placed in the hermetically sealed and ventilated desiccation box containing 1.5 L of saturated KCl solution (Supplementary Fig. S9) and desiccated for 230 min at 15°C in dim light. Temperature and relative air humidity were monitored during desiccation using data loggers (Minikin TH2, EMS Czechia). Immediately after desiccation, the biomass was washed from the filters with dH_2O and processed. The time of desiccation (t_d) 230 min was experimentally determined by subsequent calibration measurements. First, effective quantum yield Φ_{PSII} of desiccated cultures was monitored using Fluorescence Monitoring System (Hansatech instruments, UK) each 5 min during desiccation using 900 ml silica gel at 20°C, otherwise as described above, until Φ_{PSI} dropped to 0.184, and t_d for these conditions was recorded. Second, the desiccation was repeated under the same conditions with cultures on preweighed filters, which were weighed using precision balances (Kern ABP 200-5DM, Germany) in 5–10 min intervals for 2 hours. Then, the filters were dried to constant weight at 105°C and weighed to estimate the dry weight of the cultures. A calibration curve (time course of water loss) was then made and dehydration level of the cultures at the previously recorded t_d was calculated (Sigma Plot 14, Systat Software, USA). This level was then used in the following calibration using saturated KCl desiccation at 15°C to calculate t_d under these conditions (Supplementary Fig. S10).

Freeze–thaw treatment

The cultures were harvested by centrifugation (1000 g, 8 min, 15°C), the pellet was transferred to the 2 ml cryotube with dH_2O and centrifuged again (1000 g, 8 min, 15°C). The pellets in the cryotubes were then subjected to controlled freezing using a Kryo 370 freezer (Planer, United Kingdom) from 20°C to −40°C at a rate of 0.143°C min^{-1} (7 hours). The cryotubes were then immediately immersed in liquid nitrogen until further analysis. To explore recovery processes, cryotubes stored in liquid nitrogen were thawed in tap water at 40°C and processed either immediately (0 h recovery) or after being allowed to recover for 24 hours at a light intensity of 2 μmol m^{-2} s^{-1} and a temperature of 20 °C. This rapid de-frosting process is considered less harmful to microalgal cells and has been developed and tested in several algal collections (Day et al. 2007; Elster et al. 2008a, 2008b).

Cell viability test

A modification of the multiparameter dye staining protocol, originally developed for cyanobacteria by Tashyreva et al. 2013, was used (Fig. 3). The lowest concentrations of fluorescent dye that would provide effective staining were determined to overcome the potential detrimental influence on the microalgal cells. The optimal concentration of SYTOX Green was 1 μM with 30 min exposure. The final concentration of CTC (cyano-2.3-ditolyl tetrazolium chloride) was 5 mM after 30 min incubation. For DAPI staining, we followed the manufacturer's recommendations using DAPI (4.6-diamidino-2-phenylindole) at a final concentration of 5 μg ml^{-1} and an incubation time of 15 minutes. The dyes were removed by rinsing with medium to avoid excessive staining at each step.

To estimate cell viability, a series of bright-field and dark-field images (fluorescence signal of each dye) were collected using an Olympus BX52 microscope equipped with a 100 W ultra-light mercury arc lamp of the same manufacturer and an Olympus DP74 digital photographic camera (Japan). Each sample was examined in triplicate and each replicate included at least 300 cells counted in 10–15 fields of view. Images were processed using IrfanView 4.40. Cells were assigned to a specific viability status according to Tashyreva et al. (2013) with modifications (Fig. 3).

Statistical analysis of the viability test results we performed in Past 4.12b (Hammer et al. 2001). As most of the data did not pass a normality test (Shapiro–Wilk), we applied the Kruskal-Wallis one-way test at the 5% significance level to compare the percentage of viability groups between the control and experimental variants. In the same pretreatment conditions between the controls and variants in the presence and absence of nitrogen supply, and between the controls and variants with different pretreatment temperatures experiments were proceeded as well. Additionally, to estimate the difference between the controls and variants in the same pretreatment conditions we used Dunn's post hoc test at the 5% significance for the variants, which passed the Kruskal-Wallis test. Heat maps for the p-values for both tests were built in R (v. 4.3.2), using packages ggplot2 (Wickham 2016) and reshape2 (Wickham 2007).

RNA isolation and sequencing

Total RNA was extracted using RNeasy Plant Mini Kit (Qiagen, Hilden, Germany) and purified by NucleoSpin® RNA Clean-up XS kit (Macherey-Nagel, Duren, Germany) according to the manufacturer's recommendations. Transcriptomic sequencing was performed on poly(A)-enriched mRNA using the Illumina NovaSeq 6000 sequencing system (PE150) at the Cologne Centre for Genomics (Cologne, Germany). The sequence raw reads, supertranscripts, and

gene annotations for the transcriptomic study were submitted to the NCBI SRA under project number PRJNA1259228.

De novo transcriptome characterization and functional analysis

All bioinformatic analyses were performed using the Omicsbox software (v. 3.4.5, https://www.biobam.com, Götz et al. 2008). Raw reads were processed with Trimmomatic (v. 0.39; Bolger et al. 2014) and rRNA sequences were filtered out with SortMeRNA (Kopylova et al. 2012). To remove potential bacterial contaminants, Kraken 2 (RefSeq 2024-11 database) was used (Wood and Salzberg 2014, Wood et al. 2019). Furthermore, super transcripts were assembled *de novo* with Trinity (v. 2.15.1; Grabherr et al. 2011). Sequence redundancy was removed by clustering with CD-HIT (v. 4.8.1; Li and Godzik 2006, Fu et al. 2012). The completeness of the assembled transcriptome was assessed using BUSCO (v. 5.6.0) with the Viridiplantae database (Kriventseva et al. 2019, Seppey et al. 2019) and ORF analysis was performed according to Haas et al. (2013). For RNA-Seq analysis reads were aligned to the reference transcriptome using STAR (v. 2.7.8; Dobin et al. 2013) and the reads were quantified at the gene level using the HTSeq (v. 2.0.5; Putri et al. 2022). Differential gene expression analysis was conducted to assess the expression of genes under different experimental conditions with adjusted *P*-value $< .05$ (Robinson et al. 2010). To normalize the read counts between samples, the TMM (weighted trimmed mean of M-values) method was used. For each experiment, a separate experimental design was created with a selected design type (multifactorial for experiments 1 and 2, and simple for experiment 3), primary and secondary experimental and contrast conditions. Control group to determine fold changes were: 22°C + N for experiment 2, 22°C + N not desiccated (D−) for experiment 2; 22°C + N without freezing (F−) for Supplementary Fig. S6 for experiment 3 (Škuta et al. 2014). Heat maps show the normalized expression levels for each gene transformed to log2CPM. All analyses were performed using default settings, unless stated otherwise.

For annotation of the reference transcriptome, Diamond Blast searches (Buchfink et al. 2021) were performed against the NR protein database (v. 2024-11-20), restricting hits to Viridiplantae (e-value 1.0E-15). Furthermore, the transcriptome was annotated using Cloud InterProScan (v. 5.72-103.0; Jones et al. 2014) and the EggNOG Mapper (v. 2.1.0; Huerta-Cepas et al. 2019). All annotations were merged in the OmicsBox 3.4.5 software. Gene set enrichment analysis identified significantly enriched GO terms in differentially expressed gene sets (*P*-value $< .05$) (Subramanian et al. 2005). To assess the significantly regulated metabolic pathways, a Combined Pathway Analysis using the KEGG database (*P*-value $< .05$, FDR $< .05$) was used (Kanehisa and Goto 2000). Metabolic pathways were generated using mean values of expression data.

Acknowledgments

The authors would like to thank Eva Hejduková for her help during sampling on Breinosa mountain, Antonín Střížek for his help with the cultivation unit service, Leonie Agness Keilholz and Isabel Mas Martinez for their help with RNA isolation and sample preparation before sequencing, and Jana Šnokhousová for her technical assistance during the freezing experiment.

Author Contributions

A.K. performed the stress experiments, analyzed the data, and wrote the manuscript. O.B. performed the survival test, analyzed the data, and wrote the manuscript. J.K. performed the stress experiments, analyzed the data, and wrote the manuscript. L.P. identified the strain using molecular methods, performed the ITS2 secondary structure comparison, and wrote the manuscript. E.P. designed the study, analyzed the data, and wrote the manuscript. J.E. designed the study, analyzed the data, and wrote the manuscript. P.P. isolated the strain, performed the stress experiments, analyzed the data, and wrote the manuscript. B.B. designed the study, analyzed the data, and wrote the manuscript. All authors approved the final version of the manuscript.

Supplementary Data

Supplementary data is available at *PCP* online.

Conflict of Interest

The authors declare no conflict of interests.

Funding

This work was supported by the Deutsche Forschungsgemeinschaft (DFG) BE1779/25-1 (B.B., E.P.), the Czech Science foundation [project 22−08680L] and by the Czech Academy of Sciences [long-term research development project No. RVO 67985939] (J.E., P.P., A.K., O.B., J.K.) and by the University Research Centers (UNCE) at the Charles University grant no. UNCE/24/SCI/006 (L.P.). O.B. was additionally supported by the Researchers at Risk Fellowship (Czech Academy of Sciences) and the IIE Scholar Rescue Fund (IIE-SRF) Fellowship.

Data Availability

The 18S rRNA gene and ITS2 sequences of CCALA 1182 were submitted to the National Centre for Biotechnology Information (NCBI) Nucleotide sequence database (18S rRNA gene sequence: PV265869; partial 5.8S + ITS2+ partial 26S rDNA: PV275026). The sequence raw reads, supertranscripts, and gene annotations for the transcriptomic study were submitted to the NCBI SRA under project number PRJNA1259228.

References

Aigner, S., Arc, E., Schletter, M., Karsten, U., Holzinger, A. and Kranner, I. (2022) Metabolite profiling in green microalgae with varying degrees of desiccation tolerance. *Microorganisms* 10:1–18.

Arzac, M.I., Miranda-Apodaca, J., Gasulla, F., Arce-Guerrero, M., Fernández–Marín, B. and García-Plazaola, J.I. (2023) Acquisition of desiccation tolerance unveiled: polar lipid profiles of streptophyte algae offer insights. *Physiol. Plant.* 175:e14073.

Becker, B. and Marin, B. (2009) Streptophyte algae and the origin of embryophytes. *Ann. Bot.* 103:999–1004.

Becker, B., Feng, X., Yin, Y. and Holzinger, A. (2020) Desiccation tolerance in streptophyte algae and the algae to land plant transition: evolution of LEA and MIP protein families within the Viridiplantae. *J. Exp. Bot.* 71: 3270–3278.

Bolger, A.M., Lohse, M. and Usadel, B. (2014) Trimmomatic: a flexible trimmer for Illumina sequence data. *Bioinformatics* 30:2114–2120.

Buchfink, B., Reuter, K. and Drost, H.G. (2021) Sensitive protein alignments at tree-of-life scale using DIAMOND. *Nat. Methods* 18:366–368.

Curran, J., Driver, F., Ballard, J.W.O. and Milner, R.J. (1994) Phylogeny of *Metarhizium*: analysis of ribosomal DNA sequence data. *Mycol. Res.* 98: 547–552.

Day, J.G., Iorenz, M., Wilding, T.A., Friedl, T., Harding, K., Pröschold, T., et al. (2007) The use of physical and virtual infrastructures for the validation of algal cryopreservation methods in international culture collections. *CryoLetters* 28:359–376.

Dobin, A., Davis, C.A., Schlesinger, F., Drenkow, J., Zaleski, C., Jha, S., et al. (2013) STAR: ultrafast universal RNA-seq aligner. *Bioinformatics* 29: 15–21.

Dreyling, L., Schmitt, I. and Dal Grande, F. (2022) Tree size drives diversity and community structure of microbial communities on the bark of beech (*Fagus sylvatica*). *Front. For. Glob. Change* 5:858382.

Elster, J. and Benson, E.E. (2004) Life in the polar terrestrial environment with a focus on algae and cyanobacteria. In: Fuller, B, Lane, N and Benson, EE (eds) *Life in the Frozen State*. Taylor and Francis, London, UK, pp 111–149.

Elster, J., Degma, P., Kováčik, L, Valentová, L., Šrámková, K. and Pereira, A.B. (2008a) Freezing and desiccation injury resistance in the filamentous green alga *Klebsormidium* from the Antarctic, Arctic and Slovakia. *Biologia* 63:839–847.

Elster, J., Lukavsky, J., Harding, K., Benson, E.E. and Day, J.G. (2008b) Deployment of the encapsulation-dehydration protocol to cryopreserve polar microalgae held at the Czech Republic Academy of Sciences Institute of Botany. *CryoLetters* 29:27–28.

Ettl, H. and Gärtner, G. (1988) *Süßwasserflora von Mitteleuropa*, Vol. 10. G. Fischer Verlag, Jena, Germany, p 437.

Fu, L., Niu, B., Zhu, Z., Wu, S. and Li, W. (2012) CD-HIT: accelerated for clustering the next-generation sequencing data. *Bioinformatics* 28: 3150–3152.

Glaser, K., Van, A.T., Pushkareva, E., Barrantes, I. and Karsten, U. (2022) Microbial communities in biocrusts are recruited from the neighboring sand at coastal dunes along the Baltic Sea. *Front. Microbiol Sec. Terrestrial Microbiol.* 13:1–12.

Götz, S., Garcia-Gomez, J.M., Terol, J., Williams, T.D., Nagaraj, S.H., Nueda, M.J., et al. (2008) High-throughput functional annotation and data mining with the Blast2GO suite. *Nucleic Acids Res.* 36:3420–3435.

Grabherr, M.G., Haas, B.J., Yassour, M., Levin, J.Z., Thompson, D.A., Amit, I., et al. (2011) Full-length transcriptome assembly from RNA-Seq data without a reference genome. *Nat. Biotechnol.* 29:644–652.

Haas, B.J., Papanicolaou, A., Yassour, M., Grabherr, M., Blood, P.D., Bowden, J., et al. (2013) A. De novo transcript sequence reconstruction from RNA-seq using the trinity platform for reference generation and analysis. *Nat. Protoc.* 8:1494–1512.

Hammer, Ø., Harper, D. and Ryan, P. (2001) PAST: paleontological statistics software package for education and data analysis. *Palaeontol. Electron.* 4:1–9.

Holzinger, A., Lütz, C. and Karsten, U. (2011) Desiccation stress causes structural and ultrastructural alterations in the aeroterrestrial green alga *Klebsormidium crenulatum* (*Klebsormidiophyceae*, Streptophyta) isolated from an alpine soil crust. *J. Phycol.* 47:591–602.

Holzinger, A., Kaplan, F., Blaas, K., Zechmann, B., Komsic-Buchmann, K. and Becker, B. (2014) Transcriptomics of desiccation tolerance in the streptophyte green alga *Klebsormidium* reveal a land plant-like defense reaction. *PLoS One* 9:1–15.

Holzinger, A., Plag, N., Karsten, U. and Glaser, K. (2023) Terrestrial *Trentepohlia* sp. (Ulvophyceae) from alpine and coastal collection sites show strong desiccation tolerance and broad light and temperature adaptation. *Protoplasma* 260:1539–1553.

Hori, K., Maruyama, F., Fujisawa, T., Togashi, T., Yamamoto, N., Seo, M., et al. (2014) *Klebsormidium flaccidum* genome reveals primary factors for plant terrestrial adaptation. *Nat. Commun.* 5:3978.

Huerta-Cepas, J., Szklarczyk, D., Heller, D., Hernández-Plaza, A., Forslund, S.K., Cook, H., et al. (2019) eggNOG 5.0: a hierarchical, functionally and phylogenetically annotated orthology resource based on 5090 organisms and 2502 viruses. *Nucleic Acids Res.* 47:D309–D314.

Jones, P., Binns, D., Chang, H.-Y., Fraser, M., Li, W., McAnulla, C., et al. (2014) InterProScan 5: genome-scale protein function classification. *Bioinformatics* 30:1236–1240.

Kanehisa, M. and Goto, S. (2000) KEGG: Kyoto encyclopedia of genes and genomes. *Nucleic Acids Res.* 28:27–30.

Karsten, U., Herburger, K. and Holzinger, A. (2016) Photosynthetic plasticity in the green algal species *Klebsormidium flaccidum* (Streptophyta) from a terrestrial and a freshwater habitat. *Phycologia* 56:213–220.

Kiss, É., Talbot, J., Adams, N.B.P., Opekar, S., Moos, M., Pilný, J., et al. (2023) Chlorophyll biosynthesis under the control of arginine metabolism. *Cell Rep.* 42:113265.

Kopylova, E., Noé, L. and Touzet, H. (2012) SortMeRNA: fast and accurate filtering of ribosomal RNAs in metatranscriptomic data. *Bioinformatics* 28:3211–3217.

Kriventseva, E.V., Kuznetsov, D., Tegenfeldt, F., Manni, M., Dias, R., Simao, F.A., et al. (2019) OrthoDB v10: sampling the diversity of animal, plant, fungal, protist, bacterial, and viral genomes for evolutionary and functional annotations of orthologs. *Nucleic Acids Res.* 47:D807–D811.

Li, W. and Godzik, A. (2006) Cd-hit: a fast program for clustering and comparing large sets of protein or nucleotide sequences. *Bioinformatics* 22:1658–1659.

Lokhorst, G.M. (1996) Comparative taxonomic studies on the genus *Klebsormidium* (Charophyceae) in Europe. In: Jülich, W (ed) *Cryptogamic Studies*, Vol. 5. G. Fischer Verlag, Stuttgart, Germany, pp 1–135.

Manasa, S.L., Panigrahy, M., Panigrahi, K.C.S. and Rout, G.R. (2022) Overview of cold stress regulation in plants. *Bot. Rev.* 88:359–387.

Marin, B., Klingberg, M. and Melkonian, M. (1998) Phylogenetic relationships among the cryptophyta: analyses of nuclear-encoded SSU rRNA sequences support the monophyly of extant plastid-containing lineages. *Protist* 149:265–276.

Mikhailyuk, T.I., Sluiman, H.J., Massalski, A., Mudimu, O., Demchenko, E.M., Kondratyuk, S.Y., et al. (2008) New streptophyte green algae from terrestrial habitats and an assessment of the genus *Interfilum* (*Klebsormidiophyceae*, Streptophyta). *J. Phycol.* 44:1586–1603.

Mikhailyuk, T., Glaser, K., Holzinger, A. and Karsten, U. (2015) Biodiversity of *Klebsormidium* (Streptophyta) from alpine biological soil crusts (Alps, Tyrol, Austria, and Italy). *J. Phycol.* 51:750–767.

Mugnai, G., Pinchuk, I., Borruso, L., Tiziani, R., Sannino, C., Canini, F., et al. (2024) The hidden network of biocrust successional stages in the High Arctic: revealing abiotic and biotic factors shaping microbial and metazoan communities. *Sci. Total Environ.* 926:1–14.

Nagao, M., Matsui, K. and Uemura, M. (2008) *Klebsormidium flaccidum*, a charophycean green alga, exhibits cold acclimation that is closely associated with compatible solute accumulation and ultrastructural changes. *Plant Cell Environ.* 31:872–885.

Peredo, E.L. and Cardon, Z.G. (2020) Shared up-regulation and contrasting down-regulation of gene expression distinguish desiccation-tolerant from intolerant green algae. *Proc. Natl. Acad. Sci.* 117:17438–17445.

Permann, C., Stegner, M., Roach, T., Loacker, V., Lewis, L.A., Neuner, G., et al. (2024) Striking differences in frost hardiness and inability to cold acclimate in two *Mougeotia* species (Zygnematophyceae) from alpine and lowland habitats. *Physiol. Plant.* 176:e14167.

Pichrtová, M., Hájek, T. and Elster, J. (2014) Osmotic stress and recovery in field populations of *Zygnema* sp. (Zygnematophyceae, Streptophyta) on

Svalbard (High Arctic) subjected to natural desiccation. *FEMS Microbiol. Ecol.* 89:270–280.

Pierangelini, M., Ryšánek, D., Lang, I., Adlassnig, W. and Holzinger, A. (2017) Terrestrial adaptation of green algae Klebsormidium and Zygnema (Charophyta) involves diversity in photosynthetic traits but not in CO_2 acquisition. *Planta* 246:971–986.

Přibyl, P. and Cepák, V. (2019) Screening for heterotrophy in microalgae of various taxonomic positions and potential of mixotrophy for production of high-value compounds. *J. Appl. Phycol.* 31:1555–1564.

Přibyl, P., Cepák, V., Kaštánek, P. and Zachleder, V. (2015) Elevated production of carotenoids by a new isolate of *Scenedesmus* sp. *Algal Res.* 11: 22–27.

Procházková, L., Remias, D., Řezanka, T. and Nedbalová, L. (2018) *Chloromonas nivalis* subsp. *tatrae*, subsp. nov. (Chlamydomonadales, Chlorophyta): re-examination of a snow alga from the High Tatra Mountains (Slovakia). *Fottea* 18:1–18.

Pröschold, T., Marin, B., Schlösser, U.G. and Melkonian, M. (2001) Molecular phylogeny and taxonomic revision of *Chlamydomonas* (Chlorophyta). I. Emendation of *Chlamydomonas* Ehrenberg and *Chloromonas* Gobi, and description of *Oogamochlamys* gen. nov. and *Lobochlamys* gen. nov. *Protist* 152:265–300.

Pushkareva, E., Hejduková, E., Elster, J. and Becker, B. (2024) Microbial response to seasonal variation in Arctic biocrusts with a focus on fungi and cyanobacteria. *Environ. Res.* 263:120110.

Putri, G.H., Anders, S., Pyl, P.T., Pimanda, J.E. and Zanini, F. (2022) Analysing high-throughput sequencing data in Python with HTSeq 2.0. *Bioinformatics* 38:2943–2945.

Rindi, F. (2007) Diversity, distribution and ecology of green algae and cyanobacteria in urban habitats. In: Seckbach, J (ed) *Algae and Cyanobacteria in Extreme Environments*. Springer, Dordrecht, Netherlands, pp 619–638.

Rippin, M., Becker, B. and Holzinger, A. (2017) Enhanced desiccation tolerance in mature cultures of the streptophytic green alga *Zygnema circumcarinatum* revealed by transcriptomics. *Plant Cell Physiol.* 58: 2067–2084.

Rippin, M., Borchhardt, N., Karsten, U. and Becker, B. (2019) Cold acclimation improves the desiccation stress resilience of polar strains of *Klebsormidium* (Streptophyta). *Front. Microbiol. Sec. Extreme Microbiol.* 10:1–19.

Robinson, M.D., McCarthy, D.J. and Smyth, G.K. (2010) edgeR: a Bioconductor package for differential expression analysis of digital gene expression data. *Bioinformatics* 26:139–140.

Rybalka, N., Blanke, M., Tzvetkova, A., Noll, A., Roos, C., Boy, J., et al. (2023) Unrecognized diversity and distribution of soil algae from Maritime Antarctica (Fildes Peninsula, King George Island). *Front. Microbiol.* 14:1118747.

Ryšánek, D., Hrčková, K. and Škaloud, P. (2015) Global ubiquity and local endemism of free-living terrestrial protists: phylogeographic assessment of the streptophyte alga Klebsormidium. *Environ. Microbiol.* 17: 689–698.

Ryšánek, D., Elster, J., Kováčik, L. and Škaloud, P. (2016) Diversity and dispersal capacities of a terrestrial algal genus *Klebsormidium* (Streptophyta) in polar regions. *FEMS Micrologiol. Ecol.* 92:fiw039.

Seppey, M., Manni, M. and Zdobnov, E.M. (2019) BUSCO: assessing genome assembly and annotation completeness. *Methods Mol. Biol.* 1962: 227–245.

Silva, P.C., Mattox, K.R., Blackwell, W.H., Jr. (1972) The generic name *Hormidium* as applied to green algae. *Taxon* 21:639–645.

Škaloud, P. (2006) Variation and taxonomic significance of some morphological features in European strains of *Klebsormidium* (*Klebsormidiophyceae*, Streptophyta). *Nova Hedwig.* 83:533–550.

Škaloud, P. and Rindi, F. (2013) Ecological differentiation of cryptic species within an asexual protist morphospecies: a case study of filamentous green alga *Klebsormidium* (Streptophyta). *J. Eukaryot. Microbiol.* 60: 350–362.

Škuta, C., Bartůněk, P. and Svozil, D. (2014) InCHlib - interactive cluster heatmap for web applications. *J. Cheminf.* 6:1–9.

Sluiman, H.J., Guihal, C. and Mudimu, O. (2008) Assessing phylogenetic affinities and species delimitations in Klebsormidiales (Streptophyta): nuclear-encoded rDNA phylogenies and ITS secondary structure models in *Klebsormidium*, *Hormidiella*, and *Entransia*. *J. Phycol.* 44:183–195.

Staub, R. (1961) Ernährungsphysiologische Untersuchungen an der planktonischen Blaualge *Oscillatoria rubescens* DC. *Schweiz. Z. Hydrol.* 23: 82–198.

Střížek, A., Přibyl, P., Lukeš, M., Grivalský, T., Kopecký, J., Galica, T., et al. (2023) *Hibberdia magna* (Chrysophyceae): a promising freshwater fucoxanthin and polyunsaturated fatty acid producer. *Microb. Cell Fact.* 22:73.

Subramanian, A., Tamayo, P., Mootha, V.K., Mukherjee, S., Ebert, B.L., Gillette, M.A., et al. (2005) Gene set enrichment analysis: a knowledge-based approach for interpreting genome-wide expression profiles. *Proc. Natl. Acad. Sci. USA* 102:15545–15550.

Tashyreva, D., Elster, J. and Billi, D. (2013) A novel staining protocol for multiparameter assessment of cell heterogeneity in *Phormidium* populations (cyanobacteria) employing fluorescent dyes. *PLoS One* 8:e55283.

Toca, A., Oliet, J.A., Villar-Salvador, P., Maroto, J. and Jacobs, D.F. (2018) Species ecology determines the role of nitrogen nutrition in the frost tolerance of pine seedlings. *Tree Physiol.* 38:96–108.

de Vries, J. and Archibald, J.M. (2018) Plant evolution: landmarks on the path to terrestrial life. *New Phytol.* 217:1428–1434.

de Vries, J., Stanton, A., Archibald, J.M. and Gould, S.B. (2016) Streptophyte terrestrialization in light of plastid evolution. *Trends Plant Sci.* 21: 467–476.

Wang, S., Li, L., Li, H., Sahu, S.K., Wang, H., Xu, Y., et al. (2020) Genomes of early-diverging streptophyte algae shed light on plant terrestrialization. *Nat Plants* 6:95–106.

Wickham, H. (2007) Reshaping data with the reshape package. *J. Stat. Softw.* 21:1–20.

Wickham, H. (2016) *ggplot2: Elegant Graphics for Data Analysis*. Springer-Verlag, New York.

Wood, D.E. and Salzberg, S.L. (2014) Kraken: ultrafast metagenomic sequence classification using exact alignments. *Genome Biol.* 15:R46.

Wood, D.E., Lu, J. and Langmead, B. (2019) Improved metagenomic analysis with Kraken 2. *Genome Biol.* 20:257.

Xu, F. and Pan, J. (2020) Potassium channel KCN11 is required for maintaining cellular osmolarity during nitrogen starvation to control proper cell physiology and TAG accumulation in *Chlamydomonas reinhardtii*. *Biotechnol. Biofuels* 13:129.

Zhuo, H., Liu, X., Luo, S., Ou, X., Rong, X., Yang, L., et al. (2024) Physiological changes underlying increased photosynthetic-nitrogen use efficiency in response to low-nitrogen conditions in *Brassica napus* L. *Ind. Crop. Prod.* 211:118240.

Plant and Cell Physiology, 2025, 66(10),1397–1411. https://doi.org/10.1093/pcp/pcaf091, Advance Access publication on 6 August 2025, available online at https://academic.oup.com/pcp
Regular Paper